Hydrogeology Journal
https://doi.org/10.1007/s10040-024-02866-z

PAPER

Hydrogeological analysis of topography-driven groundwater flow in a low temperature geothermal aquifer system in the Julian Alps, Slovenia

Luka Serianz[1] · Anže Markelj[1] · Nina Rman[1] · Mihael Brenčič[1,2] · Judit Mádl-Szőnyi[3]

Received: 10 March 2024 / Accepted: 5 December 2024

Abstract
Groundwater flow and heat distribution was investigated in the regional karstic-fissured aquifer-aquitard system near Lake Bled in the Slovenian, eastern Julian Alps. The area features thermal springs with temperatures of 19–23 °C which are exploited by abstraction wells. The occurrence of low-temperature geothermal systems, which are common in the Alps, are associated with specific hydrogeological conditions, such as vertical hydraulic connectivity between different geological formations, relatively large elevation differences along flow paths, and the concentrated upwelling of geothermal water to the surface. The occurrence of the low-temperature geothermal field is explained by the presence of a hydraulically conductive fault along with a regional groundwater flow pattern that supports deep groundwater circulation. Hydraulic measurements and temperature data were collected from springs and wells in the area to support the analysis of flow patterns, together with the construction of a basin-scale 2D numerical flow and heat transport simulation. The diverse topographic and geological conditions result in a multi-scale groundwater flow system. The discharge of thermal waters in the Lake Bled area is a consequence of the upwelling of deep groundwater induced by a combination of the ~ 650 m difference in hydraulic head and hydrogeological heterogeneity and anisotropy, related to faulting of the geological formations. In addition, individual flow subsystems were found to significantly affect the natural heat distribution and travel times within the basin-scale system. The study highlights the combination of a basin scale approach taking into consideration local to regional-scale heterogeneities and faults in order to better understand the hydrogeological behaviour of Alpine groundwater systems.

Keywords Basin-scale groundwater flow · Thermal conditions · Carbonate rocks · Groundwater recharge · Slovenia

Introduction

The European Alpine region, known for its numerous thermal springs, offers valuable insights into deep groundwater circulation systems (Rybach 1990; Luijendijk et al. 2020). These springs indicate complex groundwater flow systems which are formed mainly as the result of topographic differences (i.e. variations in the water table) and can be described by the concept of gravity- or topography-driven groundwater flow, originally introduced by Tóth (1962; 1963). In these systems, hydraulic gradients are the main drivers of groundwater flow and thus the relationship of the groundwater table to the surface topography becomes a critical factor in shaping the flow system (Tóth 2009). The flow created by the configuration of the water table is characterized by the regional slope along with superimposed local anomalies. In addition to topography, the macroscopic heterogeneity of aquifers and aquitards is an important factor in influencing topography-driven groundwater flow in basins. On the basin-scale, the regional hydraulic conductivity of the aquifers and aquitards will influence the flow processes. Groundwater flow at the basin-scale is also influenced by climate conditions, which influence groundwater chemistry and heat transport (Freeze and Witherspoon 1967; Domenico

✉ Luka Serianz
luka.serianz@geo-zs.si

1 Geological Survey of Slovenia, Ljubljana, Slovenia

2 Faculty of Natural Sciences and Engineering, University of Ljubljana, Ljubljana, Slovenia

3 Faculty of Natural Science, Institute of Geography and Earth Sciences, Department of Geology, József and Erzsébet Tóth Endowed Hydrogeology Chair, Eötvös Loránd University, Budapest, Hungary

Published online: 03 February 2025

and Palciauskas 1973; Rabinowicz et al. 1998; Lopez et al. 2016).

Extending the concept of topography-driven flow to complex carbonate aquifer systems, recent research (Goldscheider et al. 2010; Havril et al. 2016; Mádl-Szőnyi and Tóth 2015; Mádl-Szőnyi et al. 2022) has shown that water tables in deep carbonate systems are often recharge-controlled, exhibiting a regional slope with a low degree of local topographic influence. This distinction is crucial for understanding deeper groundwater flow dynamics, where regional slope variations dictate the flow paths.

In mountainous regions, the large hydraulic head differences between recharge and discharge areas creates a sufficient potential to allow deep, warm groundwater to discharge to the surface. Since the pioneering work of Forster and Smith (1989), many modelling studies have considered the influence of groundwater on heat transport in mountainous terrain. It has been recognised that topography primarily controls advective heat transfer (forced thermal convection) in the crust (Forster and Smith 1989; Bodri and Rybach 1998; López and Smith 1995). This can also be the case in the European Alps, where the mountainous topography can feature elevation differences of 1,000 m or more at distances of only tens of kilometres. Here, groundwater flow is driven by an imposed hydraulic gradient from recharge areas located at higher elevations.

A critical aspect of understanding groundwater systems in these regions is the concept of groundwater basin delineation. Haitjema and Mitchell-Bruker (2005) and Gleeson et al. (2011) argue that identifying groundwater basins is fundamental for hydrogeological research and resource management. A groundwater basin can be defined as a given spatial unit of analysis where groundwater recharge and discharge processes can be considered together, which can facilitate a more comprehensive understanding of groundwater flow dynamics. This approach is especially relevant in complex terrains where traditional methods may overlook significant interactions between groundwater and geological structures.

In this paper groundwater flow patterns are interpretated for the aquifer system of the Julian Alps, Slovenia, from a groundwater basin perspective. This unit is expected to include groundwater processes operating at the regional scale (Tóth 2009; Jiang et al. 2018; Tóth et al. 2020). Typical analyses of groundwater basins are typically only “half-basins” that extend from a surface water divide to a valley (Tóth 1962, 1963); however, it is important to study "full-basins” (two “half” basins) due to the asymmetry of half-basins (Tóth et al. 2020; Mádl-Szőnyi et al. 2022).

If a “full-basin” approach is considered for deep a carbonate system, investigation of flow dynamics for adjacent confined and unconfined half-basins can provide answers to some basic hydrogeological questions applicable to Alpine mountainous environments (Mádl-Szőnyi and Tóth 2015; Tóth et al. 2020), These questions include: what is the geometry of the groundwater circulation system; what is the distribution of the main groundwater flow paths for different systems; how can groundwater heat transport modify the temperature-depth distribution; where does heat accumulation occur and where do thermal springs occur and what is responsible for the different chemistry and temperature observations? If these questions are answered, such answers can significantly contribute to guide more focussed hydrochemical and isotopic investigations. In addition, this can provide the basis for the planning of sustainable thermal water use. Numerous studies have highlighted the significance of groundwater circulation in mountainous landscapes and some have proceeded to model coupled heat and fluid transport processes (Vuataz 1982; Rybach et al. 1987; Rybach 1990; Biachetti et al. 1992; Gallino et al. 2009; Rybach 2009; Sonney in Vuataz 2009; Sonney 2010; Thiébaud et al. 2010; Dzikowski et al. 2016; Hilberg and Riepler 2016; Volpi et al. 2017). Over the past decade, the effects of heat transport mechanisms, including forced and/or free thermal convection, have been studied in various aquifer systems through numerical simulations and field observations (Pasquale et al. 2013; Licour 2014; Lipsey et al. 2016; Taillefer et al. 2018; Szijártó et al. 2021). Recently, Czauner et al. (2022) emphasized the relevance of a 'dynamic system approach for geofluids and their resources' for managing geofluids in geothermal groundwater systems. This framework is based on basin-scale groundwater flow systems, and underscores the importance of combining numerical, stochastic, and isotopic methods for evaluating geofluid resources and mitigating environmental impacts. This approach is particularly useful in data-sparse areas with significant variations in elevation, where numerical simulations are crucial for understanding and managing geothermal energy and groundwater resources.

The applicability of the gravity-driven groundwater flow concept was extended for deep adjoining confined and unconfined carbonates (Mádl-Szőnyi and Tóth 2015). At the basin-scale they applied the equivalent porous media (EPM) approach for numerical simulations even though these carbonate rocks are characterized by different types of permeability. Despite these simplifications, the field studies for the Buda Thermal Karst (BTK) and the derived conceptual model accurately reflected the asymmetric groundwater flow pattern between the two half-basins and resulting manifestation of the location and chemistry of thermal and lukewarm springs, karstification, heat accumulation etc. Analysis of these results was carried out using numerical simulations for different half-basin configurations (thickness of confining layer, anisotropy, heterogeneity, asymmetry of topographical driving force i.e. hydraulic gradient and direction, basinal

heat flow etc.) (Tóth et al. 2020) in order to determine the locations with the highest geothermal potential for each hydrogeologic environment.

In the Alpine region of western Slovenia four thermal springs with temperatures up to 23°C are known (Lapanje and Rman 2009). The most prominent is the Toplice thermal spring, discharging in the vicinity of Lake Bled (Slovenia) along its eastern shore. In addition to the spring, thermal water is exploited by two geothermal wells for heating and bathing. It was estimated that the total outflow of thermal water at Bled is between 60–90 l/s (Serianz et al. 2022) while only some 30–40% of it is captured; the rest remains hidden as natural discharge in the glaciofluvial sediments. In recent research (Serianz et al. 2020) chemical and isotopic analyses were carried out to identify deep groundwater circulation and recharge areas, particularly through the dissolution of carbonate minerals and isotopic signatures ($\delta^{18}O$ and $\delta^{2}H$). Hydrogeochemical investigations showed that this thermal outflow can be explained by the presence of a deeper water circulation system, with recharge occurring in the higher mountain regions, with the groundwater basin assumingly extending to the watershed divide at Mt. Triglav (Lapanje et al. 2009; Serianz et al. 2020). However, no hydraulic evidence was found to support this hypothesis.

This paper aims to evaluate the gravity-driven groundwater flow in a NW Slovenian alpine carbonate aquifer and investigate the role of thermal advection (forced thermal convection) in the unconfined confined sub-basins of the area. Groundwater flow patterns and temperature distribution were compared and evaluated based on 2D numerical simulations.

Study area

Geographic and climate settings

Bled is located in north-western Slovenia, in the Eastern Julian Alps, a mountain range of the Southern Limestone Alps (Fig. 1). This area is characterized by mountainous

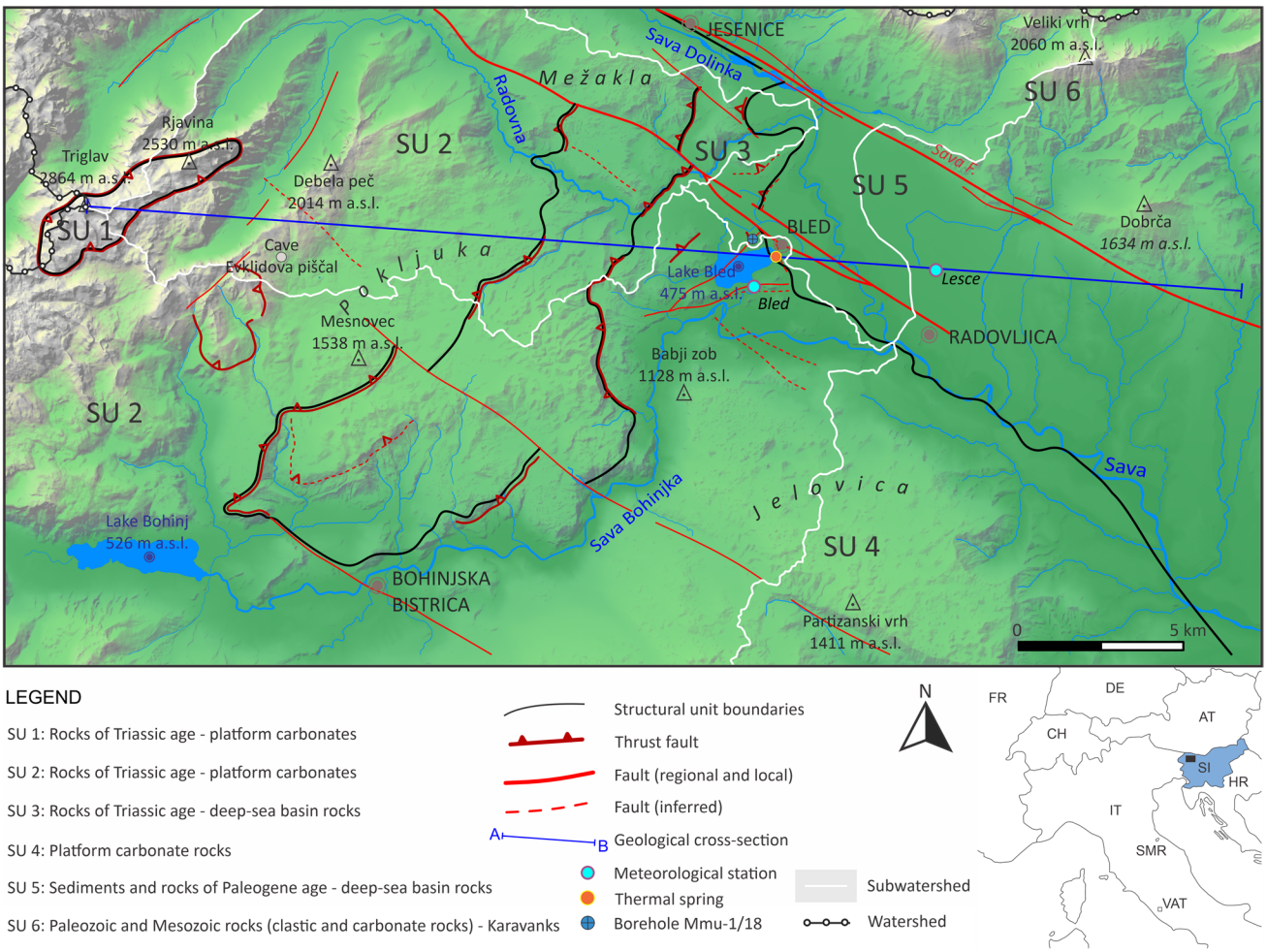

Fig. 1 Geographical settings and distribution of structural units in the study area (modified after Goričan et al. 2018)

topography, resulting in significant changes in elevation over short distances. The landscape is characterized by glaical valleys and rocky highland ridges, and peaks with specific karstic geomorphological features. The highest peak in the study area, as well as in Slovenia, is Triglav (2,864 m a.s.l.). Two large valleys in this region were formed in the Pleistocene, the Bohinj valley and the Radovna river valley. Two valleys divide the once uniform carbonate massif into three high mountain plateaus, Mežakla, Pokljuka, and Jelovica, where karstic relief predominates (e.g., Brenčič 2003). The mountain plateaus constitute an important part of the water catchment areas for both rivers, Sava Bohinjka and Radovna. Both are typical Alpine rivers and flow into the Sava River. Glacially formed Lake Bled covers an area of 1.45 km^2 and is approximately 31 m deep (Magyar et al. 2018). Recently, it receives water from small natural tributaries and artificial inflows as well as precipitation (Andrič et al. 2009). The outflow of thermal water is located on the eastern shore of the lake.

Based on data from the Archive of Weather Observation (ARSO 2021), the Alpine climate is characterized by 1576 mm average annual precipitation (period 2009–2020) in Bled and 1,523 mm in Lesce (5.5 km to the east). The average annual air temperature in this period was 10.1°C in Lesce. In the mountains the average temperature in the coldest month is −3 and 10°C in the warmest month (above 2,000 m even below 10°C). In general, most precipitation occurs in the autumn months and the least in winter.

Geological settings

The Julian Alps are part of the Eastern Southern Alps and represent a complex transition zone between the paleogeographic units of Alps and the Dinarides. Two predominant episodes of overthrusting have been recognised in the Eastern Southern Alps: A NW–SE striking and SW trending overthrust of Cretaceous and Eocene age, overlain by a younger E-W striking and S trending overthrust of Oligocene and Miocene age (Placer and Čar 1998). The Julian thrusts from bottom to top are the Krn Thrust, the Slatna Cliff and the Pokljuka Thrust at the top. Overthrust contacts are cut and displaced along younger faults (Goričan et al. 2018). The rocks of each nappe have unique stratigraphic features that allow correlation and reconstruction of the general structural setting, although today minor structural blocks lie along striking NW–SE and steep N-E trending faults.

The area consists of an alternation of predominantly carbonate rocks of Mesozoic age with some thin lenses of volcanic rocks as part of marine volcanism. Mesozoic carbonate rocks are covered by Oligocene-age sediments (marine clay) and Quaternary sediments (till, fluvioglacial sediments, and slope sediments (Goričan et al. 2018; Gale et al. 2019). The general geologic pattern is characterized by structural units overthrusted from the NW to SE deformed with later stage strike slip faults and reactivated steep reverse and normal faults (Fig. 1).

Regional scale structural units are divided into several smaller structural blocks in tectonic contacts controlled by at least two tectonic phases typical for the eastern Southern Alps. Two dominant phases of thrusting are recognized in the eastern Southern Alps: Cretaceous-Eocene striking, and SW verging thrust are overlapped by younger deformations. The present-day boundaries between units are steep NE–SW and younger NW–SE trending faults. Deformation represents Oligocene-Early Miocene NW–SE compression, Early-Middle Miocene extension, and Late Miocene to recent inversion and transpression (Goričan et al. 2018; Gale et al. 2019; Placer 1999). In the first phase, thrusting, steep reverse, and normal faults were dominant. In the second phase, faults from the first phase were either reactivated or cut and displaced with predominant strike-slip faults in the NW–SE direction (Fig. 1).

The study area is divided into six structural units/blocks – SU 1–6 (Buser 1980; Jurkovšek 1987; Placer 1999; Goričan et al. 2018; Gale et al. 2019). The Slatna Klippe (SU 1) represents overthrusted rocks of the Triglav Massif and is in tectonic contact with surrounding platform carbonates (Jurkovšek 1987; Goričan et al. 2018). The rocks of the Krn Nappe, part of the larger Julian Nappe, cover the largest area (SU 2). Considering the correlation of stratigraphic features of Mesozoic platform carbonates structural blocks SU 2 and SU 4 show generally similar features with some discontinuities in sedimentation. Between these two structural blocks, the basin rocks of the Pokljuka Nappe (SU 3) outcrop. These rocks formed during the Middle and Upper Triassic and Jurassic (Šmuc 2005; Goričan et al. 2018). Carbonate sequences of SU 3 and SU 2 are characterized by steep thrust faults and lateral strike-slip faults. The Paleogene basin sediments (SU 5) covers a large area stretching to the East and South-East outside the studied area. Regional extensional conditions in the Paleogene, followed by volcanic activity in the surrounding area resulted in locally thick deposits of pyroclastic sediments ("Peračiški tuf") with lateral transition into predominantly sedimentary formations. Due to the lack of deep structural data the geometry of contact and the features of the bedrock of the SU 5 are not yet fully known. It could consist of basin rocks of the Pokljuka Nappe (SU 3) or be overthrusted onto rocks of the carbonate platform (SU 2/SU 4). The structural block of the Karavanke (SU 6) extends north of the Sava fault zone and is not thought to influence groundwater flow in

the area (Atanackov et al. 2021). The boundary between SU 6 and other structural units is characterized by the Sava fault, which represents a regional scale transpressive and strike-slip fault (Placer 1996).

Quaternary sediments partially cover these formations due to the activity of glaciers extended along the Alpine valleys. Some till deposits can be found at the Pokljuka plateau in the south. Glacial activity and postglacial fluvial processes led to the formation of up to tens of meters of Quaternary sediments deposited in terraces, reflecting several glacial-interglacial events (Bavec and Verbič 2004; Serianz 2016). Slope sediments are the youngest, covering large areas in the mountains and differing in thickness and composition, with carbonate gravel predominating. Clay and silt deposits are found in the vicinity of Lake Bled, which were deposited during glacial and interglacial periods due to the varying extent of the lake.

Applied numerical method

Approach

The basin-scale groundwater flow conditions were explored by numerical simulation along a 2D section from the Triglav (western part) crossing Lake Bled as far as the eastern part of the study area. The scale of the section is 2–4 km (depth) × 35 km (length).

The heterogeneity of the karstic-fissured aquifer, hydraulic conductivity, and flow regime can introduce numerous issues and uncertainties at the local scale. However, due to the adjustment of the regional groundwater flow concept these can be eliminated at the first approximation. During numerical simulations, the whole carbonate aquifer system or groundwater basin with its confined and unconfined parts as a whole was considered as opposed to a single aquifer (Mádl-Szőnyi and Tóth 2015; Tóth et al 2020; Mádl-Szőnyi et al. 2022). Assuming that the size of the basin is several orders of magnitude larger than the size of karst channels and fissures, the entire basin can be treated as a continuum, which is why the EPM approach can be applied (Scanlon et al. 2003; Kuniansky 2016; Havril et al. 2016 etc.). Here, hydraulic continuity plays the main role, assuming a groundwater flow through different geological formations, which is a consequence of the spatial distribution of the fluid potential (Hubbert 1940). Hydraulic continuity can be assumed if the vertical and horizontal hydraulic connectivity of geological formations is known a priori. Hydraulic continuity is theoretically defined by Tóth (1995) as the ratio of the induced change in the hydraulic head (or pore pressure) to the inducing change of the hydraulic head (or pore pressure):

$$C = \frac{\Delta\psi_2}{\Delta\psi_1} = \frac{\Delta h_2}{\Delta h_1} \tag{1}$$

where C is continuity, $\Delta\psi$ pressure head change, Δh hydraulic head change, subscript 2 refers to induced change and subscript 1 to the inducing change. Herein, the basin scale approach was used in the numerical simulations of 2D groundwater flow, namely by assuming a continuous groundwater flow for two connected sub-basins.

Governing equation

In this study, the numerical models with combined heat transfer and groundwater flow were solved with FEFLOW 7.2 software (Diersch 2013). The model uses finite element analysis to solve the groundwater flow equation of both saturated and unsaturated conditions as well as mass and heat transport. The governing equation describing the fluid flow in the reservoir can be expressed as follows (eg. Bear 1972; De Marsily 1986; Domenico and Schwartz 1998):

$$n\frac{\partial\rho_w}{\partial t} + \nabla\cdot\left(\rho_w \mathbf{v}_D\right) = 0 \tag{2}$$

where n is porosity, ρ_w is density of water, t is time and $\mathbf{v}_D$ is Darcy flow velocity vector described for a single phase flow as:

$$\mathbf{v}_D = -\frac{k}{\mu}(\nabla P - \rho_w g \nabla z) \tag{3}$$

where k is the intrinsic permeability of the porous medium, μ is dynamics viscosity, g is the acceleration due to gravity, z is the vertical coordinate and P is the pore pressure. The intrinsic permeability is a property of the solid material describing its ability to conduct water. In practice, the term K saturated hydraulic conductivity is more often used.

$$K = kg\frac{\rho_w}{\mu} \tag{4}$$

In a fully saturated medium, the macroscopic energy balance equation for the solid phase can be described using the convection-conduction equation (eg. Nield and Bejan 2017):

$$\left[\left(n\rho_w c_w + (1-n)\rho_s c_s\right)\frac{\partial T}{\partial t} + \rho_w c_w \mathrm{v}_D\cdot\nabla T\right] = \nabla\cdot(\lambda\cdot\nabla T) \tag{5}$$

where n is porosity, $\rho_w c_w$ and $\rho_s c_s$ are the volumetric heat capacity of water and solid, respectively, T is temperature, t is time and λ *is* the thermal conductivity which is described in terms of a local volume average, as:

$$\lambda = (1-n)\lambda_s + n\lambda_w \tag{6}$$

where λ_s and λ_w are the thermal conductivities of porous media and water, respectively.

Additionally, the volumetric heat capacity of the saturated medium, ρc, can be written as:

$$\rho c = n\rho_w c_w + (1-n)\rho_s c_s \tag{7}$$

Steady-state fluid flow and heat transfer modules were applied assuming constant fluid density, dynamic fluid viscosity and gravitational acceleration. In this manner, conduction and advective thermal convection (coupled via the Darcy velocity) were the only sources of heat transfer. The relative importance of heat conduction and convection can be described with the nondimensional Peclet number, which can be described as the relation between advective heat flow and heat conduction, along the characteristic length L (Al-Khoury 2012):

$$\mathrm{Pe} = \frac{\rho_w c_w \mathbf{v}_D L}{\lambda} \tag{8}$$

At low values of Pe (Pe < 1), conduction predominates, while convection became significant at higher values of Pe (Pe > 1). In this paper, groundwater circulation is expected to be affected only by forced convection. The potential of free convection was not examined due to the low geothermal gradient.

Hydrogeological background of the numerical simulations

Delineated sub-basins and model domain

Geological and topographic conditions were evaluated along a 2D section from the mountainous area in the west, crossing Lake Bled and continuing to the eastern part of the study area (Fig. 1). Based on the topography and geology, two hydrogeological sub-basins were defined (Fig. 2a). The first extends from Mt. Triglav (groundwater divide located at distance 0 km; elevation 2864 m; elevation of water Table 1310 m) as far as the deepest elevation at Sava Dolinka River (distance 22.9 km; elevation 428 m; elevation of water level 427 m). The eastern sub-basin extends from Sava Dolinka at the eastern end of the section (distance 35.1 km; elevation 562 m; elevation of water level 561 m). Lithostratigraphic conditions vary along the section, where the western sub-basin is represented by interconnected aquifers with karstic-fissured porosity and predominantly unconfined conditions.

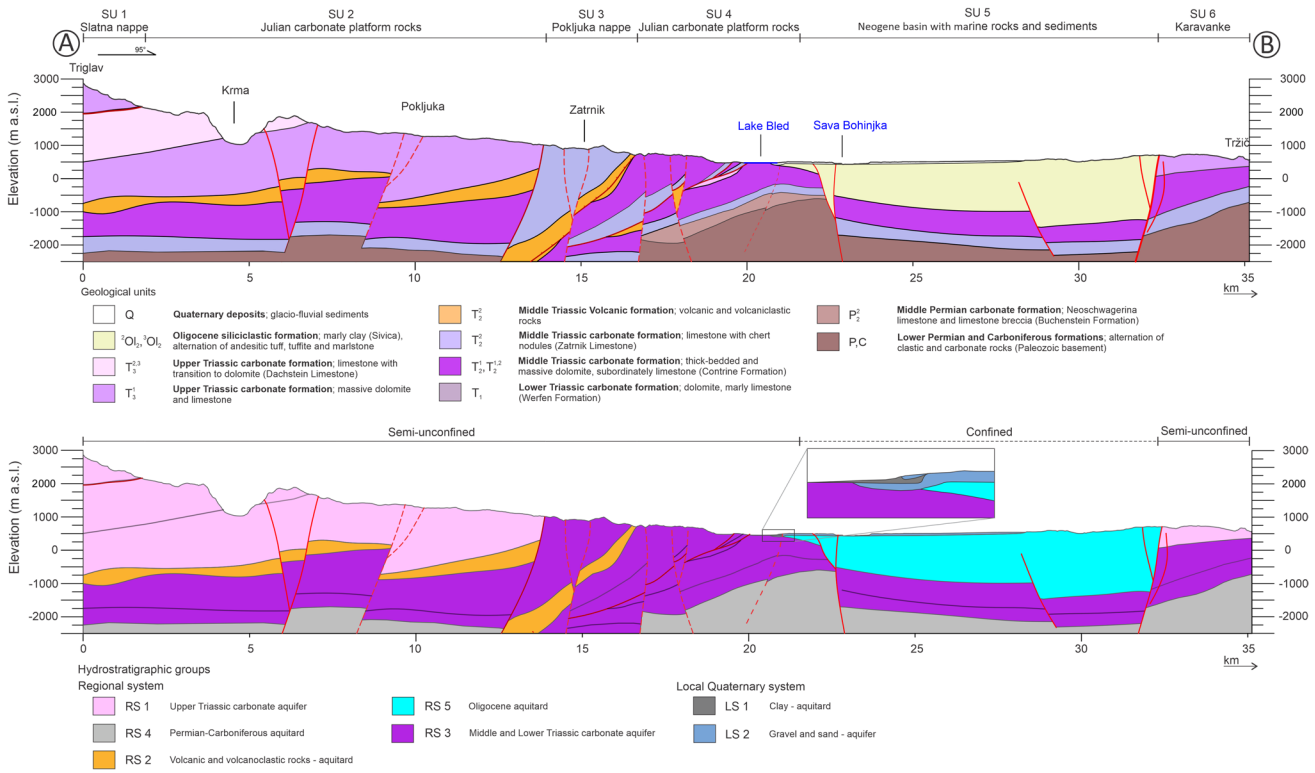

Fig. 2 Geological units (top) and hydrostratigraphic groups (bottom) in a WNW-ESE cross-section

Hydrostratigraphic units

For groundwater flow simulations, the geological cross-section was converted into a hydrostratigraphic cross-section, where several units are distinguished (Fig. 2b): Upper Triassic carbonate aquifer (RS 1), volcanic rocks (RS 2), Middle and Lower Triassic aquifer (RS 3), Permo-Carboniferous aquitard (RS 4), and Oligocene aquitard (RS 5) (Table 1, Fig. 2b). Additionally, for the surroundings area of the thermal water outflow, a local outflow model was added to the model to represent a clay aquitard (LS 1) and sandy gravel aquifer (LS 2).

The hydraulic parameters for each hydrostratigraphic unit were determined using field data and literature compiled in the archives of the Geological Survey of Slovenia. These values were validated against regional data to ensure their accuracy. Due to the pronounced heterogeneity in karstic-fissured rocks, hydraulic conductivity varies significantly (Tab. 1). For instance, higher hydraulic conductivities were assigned to fractured carbonate units, while lower values were applied to finer-grained sediments. According to fieldwork investigations and Verbovšek (2008), the average hydraulic conductivity (K) in carbonate rocks of the Triassic formation is in the order of 1×10^{-6} m s^{-1} with strong heterogeneity due to the effects of matrix, fractures, and channels. In Permian and Permo-Carboniferous basement rocks, the anisotropy is more significant than in the carbonate layers. Representative hydraulic conductivity is estimated at 1×10^{-7} m s^{-1}. Oligocene marine sediments deposited in the Bled basin have the lowest hydraulic conductivity at $<1\times10^{-9}$ m s^{-1}. Quaternary sediments mainly consist of gravel, sand, and clay and represent a siliciclastic aquifer that covers the carbonate layers and Oligocene clay sediments.

Recharge conditions and consequent regional groundwater level

The water table configuration in the cross section A-B is divided into four separate segments, which include the karstic-fissured aquifer (KFA), the Quaternary aquifer (QA) and the Oligocene clay (OC) (Fig. 3). The exact groundwater table configuration is unknown for the carbonate system. A large part of the groundwater from the Pokljuka Plateau most likely flows towards Sava Bohinjka and into the Krma alpine valley which feeds into the Radovna River Valley (Fig. 1). The only information on groundwater levels in this area is available from a cave named "Evklidova piščal", which reaches a depth of 429 m below ground level (bgl) with a siphon at an elevation of 1,121 m a.s.l. (Kranjc 2016). This siphon represents the only point at which the upper phreatic zone of the aquifer that was observed and represents important datum for estimating the distribution of groundwater levels in the entire Pokljuka karst massif. At the eastern boundary of the massif, groundwater discharge occurs near Lake Bled, where the elevation of the lake water level is 475 m a.s.l. In the permeable Quaternary deposits the water table configuration is more constrained and was determined using data collected from local wells (drinking water supplies, groundwater heat pumps, thermal wells etc.), observation wells, and springs. The water table in the Oligocene group (RS 5) was determined from the surface elevation and the average depth (1 m bellow surface).

For the comparison and validation purposes of water budgets in the hydraulic model, recharge conditions were estimated through the deterministic water balance model mGROWA-SI based on raster data for the standard observation period from 1981 to 2010 (Andjelov et al. 2016). The model separates direct runoff and groundwater recharge. The latter is calculated using base flow indices (BFI) which describe base flow as a constant fraction of the total runoff. The recharge conditions in the study area are very heterogeneous. According to the mGROWA-SI model the groundwater recharge in the mountainous area can be as high as 1500 mm, whereas in the lowlands, the groundwater recharge can be less than 200 mm. For the purpose of this paper the average groundwater recharge (R') for the Sava Bohinjka and Radovna watersheds was calculated to be 763 mm from the mGROWA-SI model outputs. Both watersheds were taken into account since they are intersected by the same cross section (Fig. 2).

Table 1 Summary of hydraulic and thermal input parameters for simulations

Geological unit	Hydrostratigraphic unit	Hydraulic behaviour	K (m s^{-1})	n (%)	$c_s\rho_s$ (MJ m^{-3} K^{-1})	λ_s (J m^{-1} s^{-1} K^{-1})
P_2^2, PC	RS4	Basement	1×10^{-7}	5	2.5	2.0
T_2^1, $T_2^{1,2}$,T_2^2	RS3	Aquifer	5×10^{-6}	1	2.3	3.5
T_2^2	RS2	Aquitard	1×10^{-7}	1	2.2	2.1
$T_2^{2,3}$, T_3^1	RS1	Aquifer	1×10^{-6}	1	2.2	3.0
$^2Ol_2$, $^3Ol_2$	RS5	Aquitard	1×10^{-9}	25	4.4	1.4
Q (clay)	LS1	Aquitard	1×10^{-9}	30	4.4	1.4
Q (sandy gravel)	LS2	Aquifer	3×10^{-5}	20	2.4	1.6

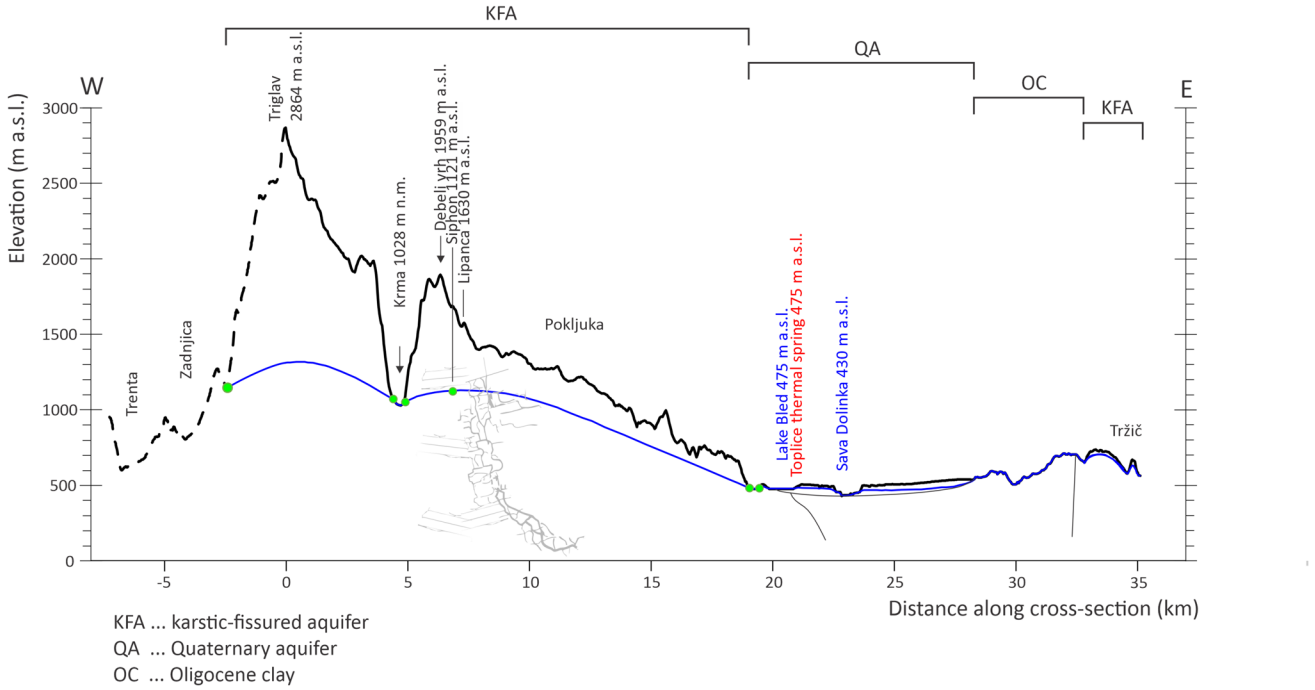

Fig. 3 Groundwater level along the hydrogeological cross section A-B in different segments (green dots: known groundwater level elevation points; blue line: estimated water table)

Thermal properties

Thermal properties of the main lithological units in the wider area of Bled were determined using thermal conductivity optical scanning (TCS) analysis of rock samples (Rajver and Adrinek 2023). The average measured thermal conductivity of carbonate rocks was between 3.0 and 3.5 W m^{-1} K^{-1}. Lower values occur for piroclastic rocks, with the average thermal conductivity for tuff at 2.4 W m^{-1} K^{-1}. The lowest thermal conductivity was measured in sediments, namely sand clay of Oligocene age with a value of 1.4 W m^{-1} K^{-1} (Table 1).

In Bled, data for undisturbed groundwater temperature is only available for a 150 m well Mmu-1/18 (drilled in Anisian dolomite – T_1^2) (Fig. 1). Two wells were logged using Robertson Geologging equipment. The first log was collected on April 2018, a few days after drilling was completed and the second log was collected in February 2020. Extrapolating the temperature to a depth of zero and the measured temperature gradient in the lower part of the well provided a geothermal gradient of 11 °C km^{-1} (Fig. 4b). The low geothermal gradient is compatible with existing estimations and is related to the low heat flow density of approximately 38 mW m^{-2} (Rajver 2018) (Fig. 5).

Model domain, boundary conditions and parameters and simulation scenarios

The finite element method used in this model was based on discretising the model domain into triangular elements. Model domain length and depth are 35.1 km and 5 km (max. height), respectively. Since the quality of the results is significantly affected by the type of the elements and their distribution within the model domain, 10 m refinement was done near the geological boundaries. In the numerical modelling, the hydraulic effects of faults were ignored since it was assumed that only the contacts of the formations/units with different hydraulic conductivity influence the model.

Groundwater table configuration was prepared with point geometry and used as a fixed upper boundary condition for the fluid flow, as the goal of this simulation was to determine the flow pattern and its thermal effects as opposed to the fluxes, much like the approach applied by Tóth et al. (2020) and Szijártó et al. (2021). This study applied a spatially-varying hydraulic head as the top boundary condition in order to ensure a close to realistic water table (Fig. 6). This approach eliminates the need to determine spatial groundwater recharge rates but may potentially produce unrealistic groundwater recharge rates

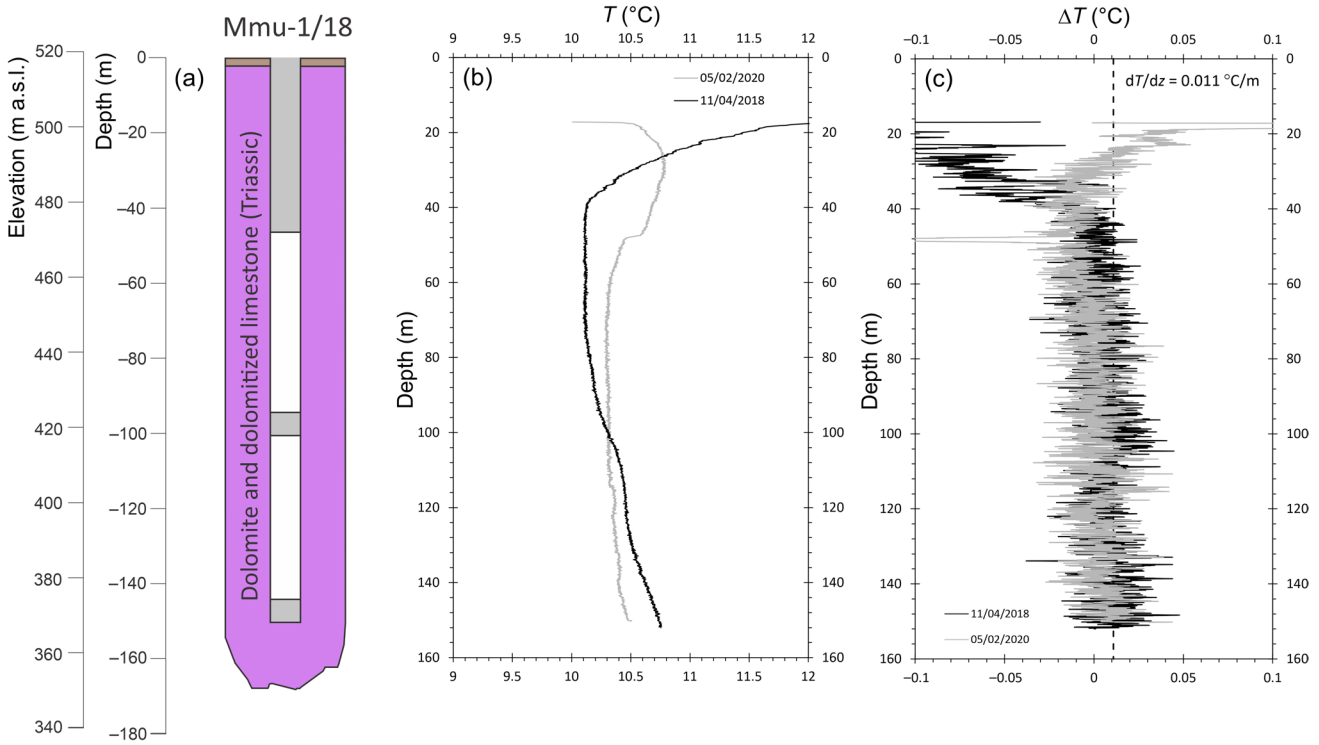

Fig. 4 Lithological profile (**a**), temperature gradient (**b**) and differential temperature—difference in temperature between two vertical points in a well (**c**) by logging in borehole Mmu-1/18 with wellhead at 518 m a.s.l

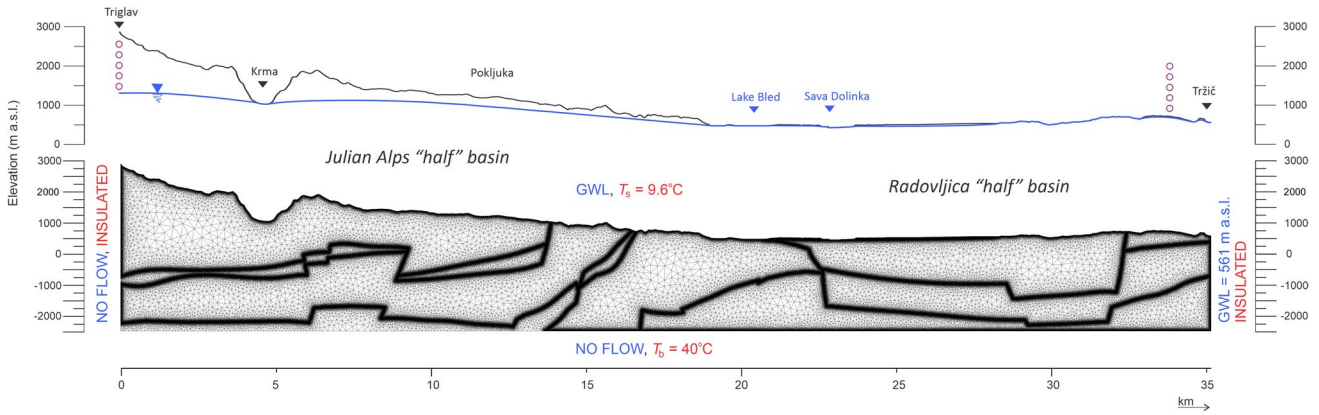

Fig. 5 Geometry of the model domain of A-B cross section with boundary conditions. GWL: groundwater level

that are much larger than precipitation (Dai et al. 2021). Therefore, the numerical results were validated by comparing the calculated recharge rate (R) and the estimated annual recharge (R') calculated using the mGROWA-SI model: R/R' expressed in %.

The model domain of the coupled half-basins has a fixed groundwater level condition (561 m a.s.l.) at the right boundary and a no flow condition at the left and bottom boundaries (Fig. 6). The elevation of the base of the model is −2500 m a.s.l., where the low permeability Permo-Carboniferous aquitard is probably dominant. Heat transfer boundary conditions are determined as insolated on the left and right side of the model domain. The upper boundary was determined as isothermal with a fixed groundwater temperature of 9.6 °C, which is the average annual temperature for the average elevation of the model

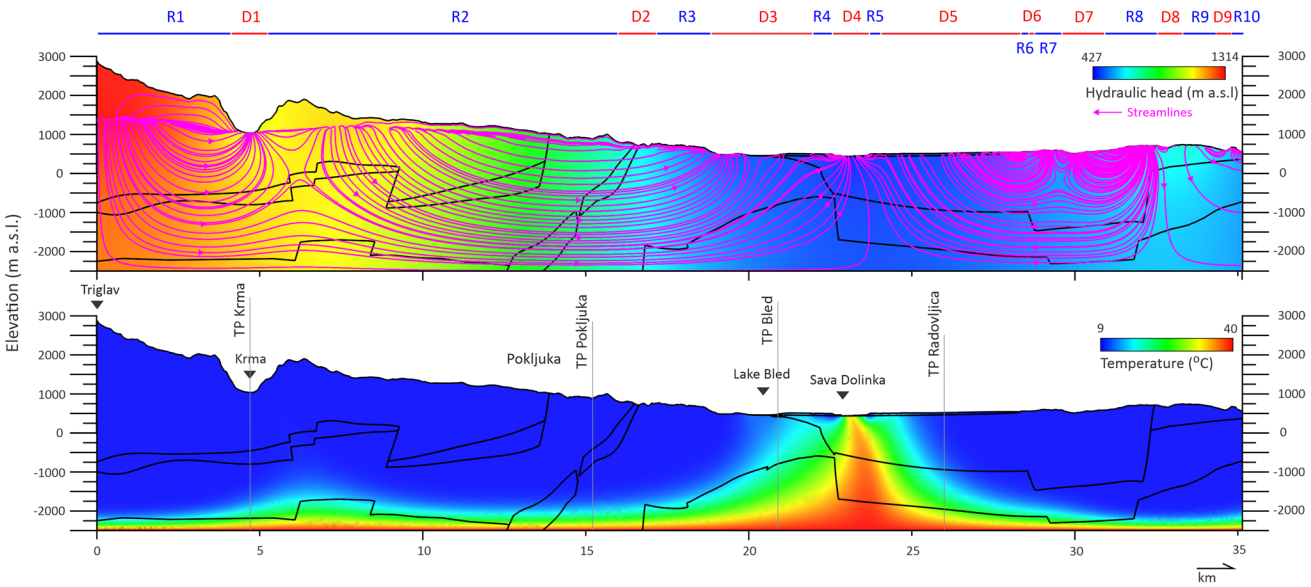

Fig. 6 Groundwater flow and heat transport simulations for S1 homogenous and isotropic conditions (vertical exaggeration is 1:1.2)

Table 2 Values of constant parameters applied in numerical simulations

Symbol	Unit	Value
T_s	°C	9.6
T_b	°C	40
$c_w\rho_w$	MJ m^{-3} K^{-1}	4.2
λ_w	J m^{-1} s^{-1} K^{-1}	0.60
G	m s^{-2}	9.81

domain (Table 2). The lower boundary is also isothermal, determined by a fixed temperature of 40 °C, which is the expected temperature according to the site-specific geothermal gradient. The model simulations therefore examine a no-flow and thermally insulated (western boundary) versus a hydrostatic pressure and insulated (eastern boundary) boundary condition which is assumed to be the most realistic condition in this study area.

For comparison, three scenarios S1: homogenous and isotropic, S2: heterogenous and isotropic, and S3: heterogenous and anisotropic are assumed and examined for the cross section (Table 3) with various input data for the calculations, where some parameters remained constant. Specific averaging values for model simulations for $c_s\rho_s$ were evaluated based on literature (VDI 2012).

Results

Simulated flow and temperature distribution

Homogenous model – S1

The homogenous model aimed to represent the effect of the natural boundary conditions on flow and temperature distribution. In addition to visualize the distribution of the different flow systems (local, intermediate and regional). The left side of the model represents the effect of the surface and subsurface divide at Triglav. Here, the hydraulic gradient is greater relative to the right side of the model (Fig. 6). In addition, the total area of local systems flowing toward the center of the basin is significant. The homogenous model well illustrates the manifestation of the local flow component discharging at D1 and the regional flow components discharging at D3 and D4 (Fig. 6), all originating from R1

Table 3 Estimated model parameters in three different scenarios for cross-sections

Scenario	Parameters			
	K (m s^{-1})	n (%)	$c_s\rho_s$ (MJ m^{-3} K^{-1})	λ_s (J m^{-1} s^{-1} K^{-1})
(S1) Homogenous and isotropic system	1×10^{-6}	1	2.5	2.5
(S2) Heterogenous and isotropic ($K_x/K_z=1$)	values are given in Table 1			
(S3) Heterogenous and anisotropic ($K_x/K_z=0.1$)	values are given in Table 1			

recharge section. The homogenous condition allows for deep groundwater circulation (more than 2 km deep) within the regional groundwater flow system, whereas the maximum depth of groundwater circulation is 1.5 km for the local groundwater flow system. There is a low number of local flow systems at the left side of the model, where the topography is less pronounced. D1 and D2 represent the discharge of the local groundwater flow component from the left side of the model. On the right side of the model, the discharge of the local groundwater flow component is represented by D6–D9. The calculated R for the S1 scenario was 875 mm and the recharge rates $R/R' = 87\%$, which is a satisfactory result.

In a homogeneous and isotropic system, the influence of forced thermal convection, which includes the advection and conduction mechanisms of heat transfer, on the temperature distribution is shown in Fig. 6. Due to the isothermal boundary conditions at the top of the model, water enters the system at 9.6 °C. In a recharge area with higher elevation, the effect of cold water inputs propagates to the bottom of the model. This is due to the relatively good permeability of the Triassic aquifers and the high hydraulic gradient resulting from the high elevation differences. On the other hand, a positive and concentrated temperature anomaly develops in the outflow area near the Sava Dolinka River, representing the lowest elevation along the section, where thermal groundwaters approaches the model surface at a temperature of approximately 30 °C.

Heterogenous and isotropic model – S2

In the S2 model scenario hydrogeological conditions are defined by the specific permeability, porosity, and the thermal property values of the various geological materials (Table 1). The model results show the pronounced influence of water flow between the different hydrostratigraphic units (Fig. 7a), which are manifested in the bending and sloping of streamlines as they pass through the less permeable layers. In each individual hydrostratigraphical unit, streamline density increases where the thickness of the hydrostratigraphical unit decreases. The isotropic model illustrates the manifestation of the local flow component discharging at D1 or D2 and the regional flow component discharging at D3 (Fig. 7a), all originating from R1 recharge section. The isotropic condition allows groundwater to circulate at depths of around 1 km, even within the local groundwater flow system. This scenario also indicates the formation of a groundwater flow system in the Oligocene aquitard that recharges from R4, R5, and R6 (Fig. 7a), although the depths of the local flow systems are not as deep compared to the homogenous scenario. Similar to S1, the number of local flow systems on the left side of the model, in the areas where topography is less pronounced, are fewer relative to the right side of the model. The calculated R for S2 was 1632 mm and the recharge rates $R/R' = 47\%$, which is probably a conservative estimate.

Peclet number simulations suggest that convection mostly occurs in limestone and dolomite layers of hydrostratigraphic units RS 1 and RS 3. In the right half-basin of the model, higher Peclet numbers ($Pe > 1$) also occur in RS 3 below the confined part. The thermal and hydrogeological properties of the aquitards and siliciclastic layers, do not allow for higher Peclet numbers. As with S1 simulations, it can be observed that heat becomes concentrated in the middle part of the model, near the lowest elevation area where the flow systems of the sub-basins are discharged. The influence of the isothermal upper boundary conditions is also similar to S1. The downward flow of the recharging cold water down to a depth of a few 1,000 m bgl creates a cooling effect. Since $K_z = K_x$, the occurrence of groundwater with elevated temperatures at the bottom of the model corroborates with simulated temperature profiles at Krma (at 4.7 km distance – Fig. 8a) and Pokljuka (at 15.2 km distance – Fig. 8a). A positive temperature anomaly develops in the outflow area near Lake Bled, which is approximately 2 km west compared to the S1 scenario. Here the simulated thermal water approaches the model surface at a temperature of approximately 22 °C. This temperature represents a value estimated from the simulated temperature profile (Fig. 8c). On the eastern side of the model, the temperature distribution is also influenced by advective cooling due to the topography-driven groundwater flow.

Heterogenous and anisotropic model – S3

In general, the permeability of geological formations is typically anisotropic and thus has different magnitudes in three coordinate directions, $K_x \neq K_y \neq K_z$. When modeling groundwater flow, the vertical permeability is assumed to be of an order of magnitude lower than the horizontal one ($K_z/K_x = 0.1$). As can be seen from the simulations, the anisotropy increases the flow in the direction of higher permeability (Fig. 7b). Similar to S2, the S3 model results show the pronounced influence of different hydrostratigraphic units on groundwater flow paths, manifested by the bending and sloping of the streamlines through less permeable layers. The anisotropic model, like S2, illustrates the manifestation of the local flow component discharging at D1 or D2 and the regional flow component discharging at D3 (Fig. 7b), all originating from the R1 recharge section. In the case of R1/D1, the anisotropic conditions limit the circulation of the local groundwater system to a depth of less than 200 m below the groundwater table (Fig. 7b). In the eastern part of the model, local groundwater flow is recharging at R4, R5, and R6 but it is less significant than in case of S2. Similar to S1 and S2, the number of local flow systems on the left

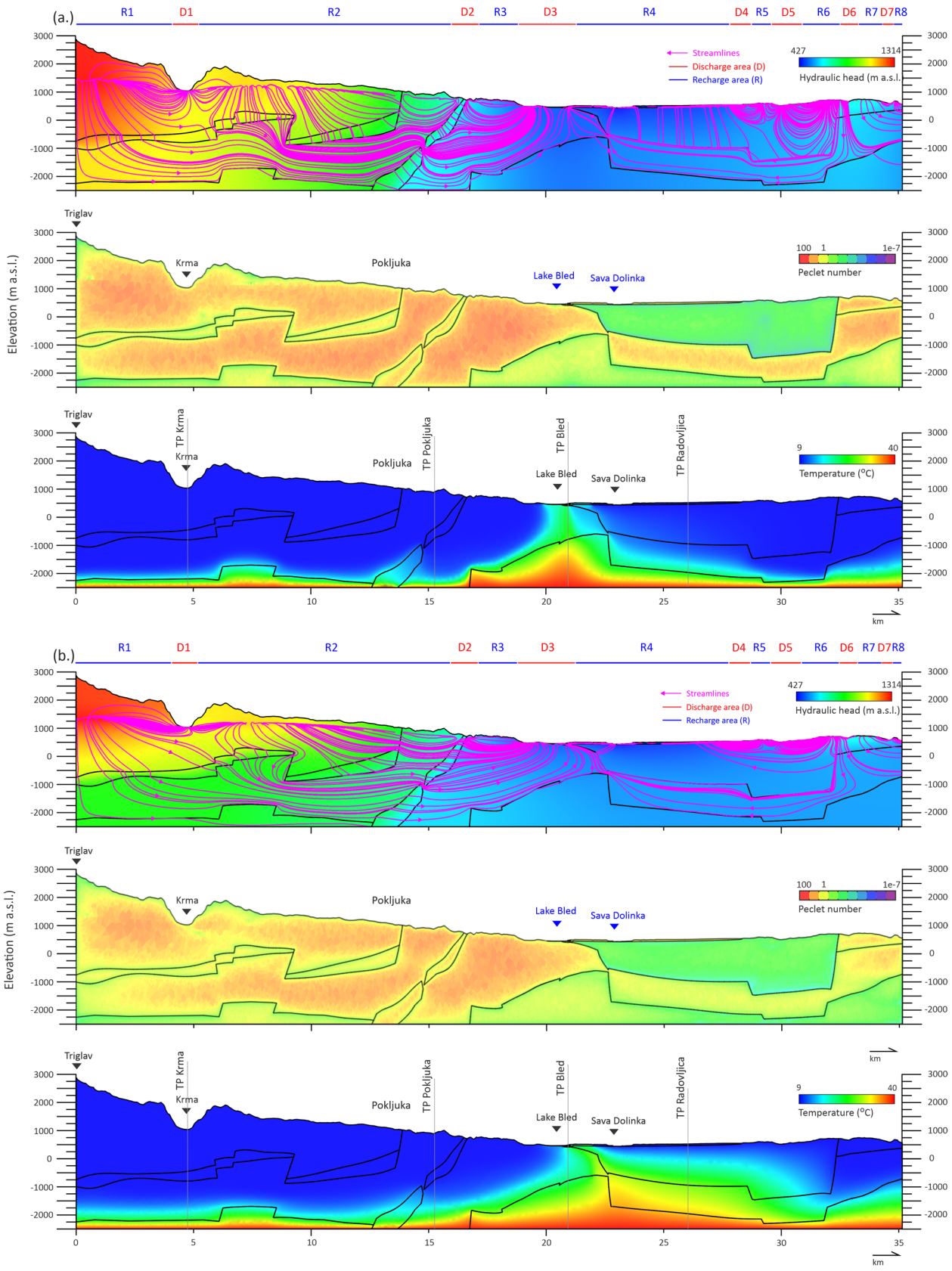

Fig. 7 Groundwater flow, Peclet number, and heat transfer simulations for (**a**) heterogenous and isotropic – S2 and (**b**) heterogenous and anisotropic conditions – S3 (vertical exaggeration is 1:1.2)

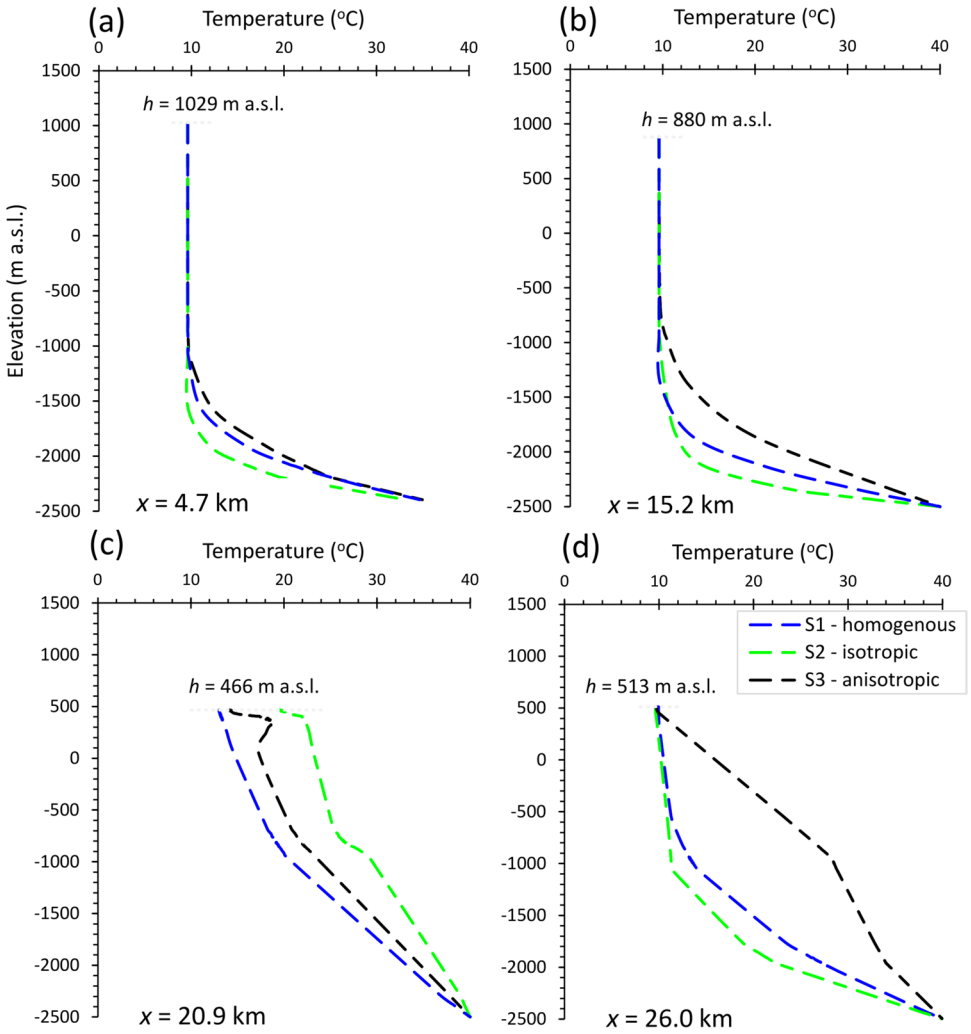

Fig. 8 Calculated temperature profiles at different locations along the simulated cross section Krma (**a**), TP Pokljuka (**b**), TP Bled (**c**) and TP Radovljica (**d**) for the three scenarios (S1, S2, and S3)

side of the model, in areas where the topography is less pronounced, is lower than on the right side of the model. The calculated R for the S3 was 788 mm and the recharge rates $R/R' = 97\%$, which is a very good estimate.

As can be seen from the Peclet number simulations, similar to S2, convection mostly occurs at the left site of the model, in the Triassic limestone and dolomite layers, represented by hydrostratigraphic units RS 1 and RS 3. However, at the right site of the model, low Peclet numbers ($Pe < 1$) occur in RS 3 below the confining layer. In other layers, the groundwater flow rate is too low to allow favourable Peclet numbers to be established. In the recharge area, heat is concentrated along the bottom of the model to a greater extent than in the other two scenarios, which is also suggested by temperature profiles at Krma (4.7 km – Fig. 8a) and Pokljuka (15.2 km – Fig. 8b). Advective transport of heat by groundwater lowers temperatures near the higher recharge areas and raises temperatures near Lake Bled, where thermal groundwaters approach the model surface with a temperature of approximately 18.6 °C. This value represents the temperature of upwelling fluid and was estimated from the temperature profile (Fig. 8c). At the confined part (RS5), the temperature profile also shows accumulation of heat in the model below 0 m asl (Fig. 8d). According to the simulation results, scenario S3 seems the most realistic scenario for the study area.

Simulated travel time

The simulated age of groundwater can be defined as the time that has elapsed since the water entered the saturated zone (Bethke and Johnson 2008). Here, the simulation of groundwater age through numerical modelling is based on the velocity field derived from the groundwater flow model and assumes that the conservative tracer travels along flow paths without mixing. Local systems are on the order of about 10 years at most. Residence time is longer for the S3 scenario relative to the S2 scenario, since the horizontal flow component dominates over the vertical one (Fig. 9; S3). For comparison in Fig. 9, the representative regional streamline

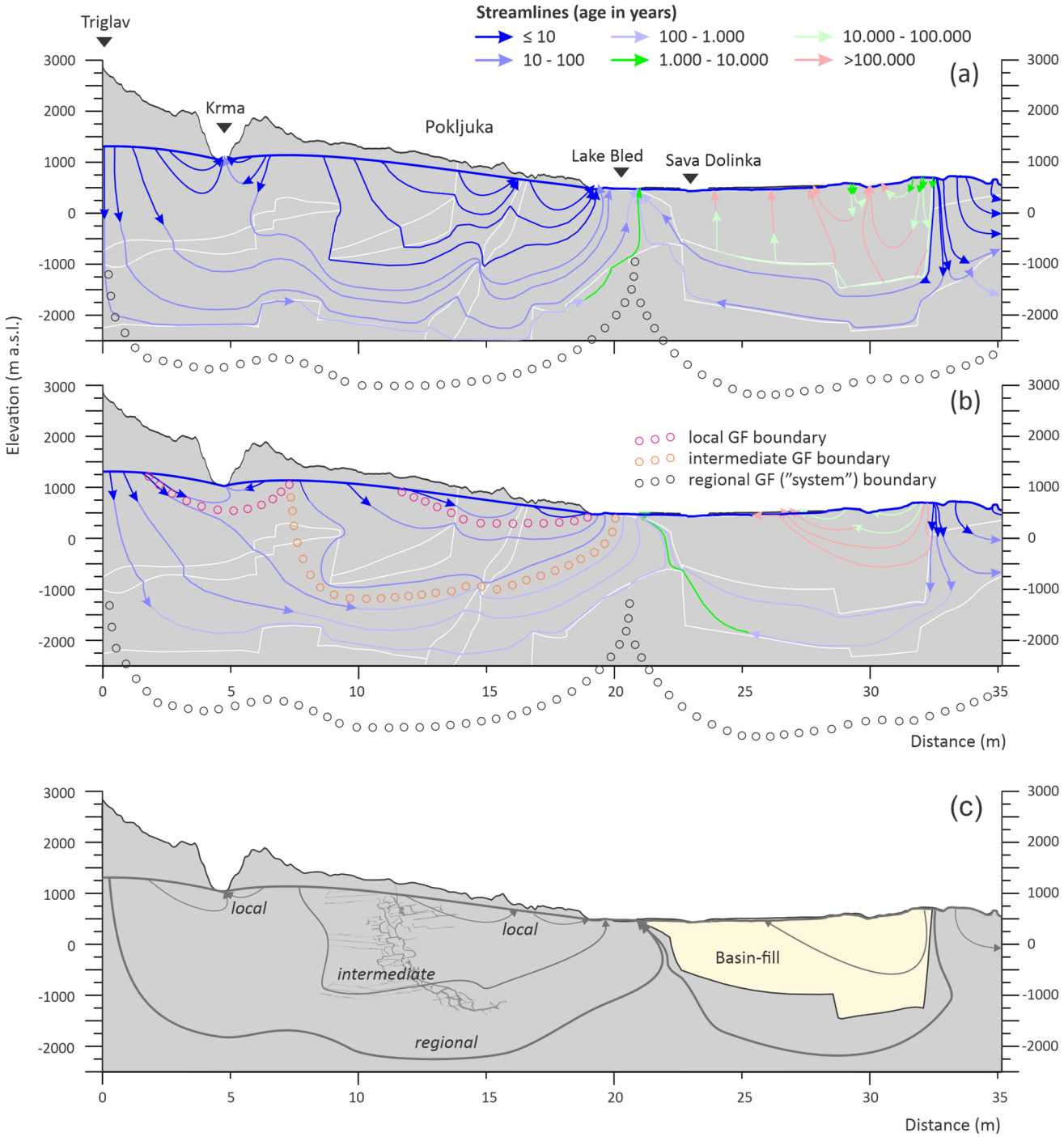

Fig. 9 Trajectories of particles following the velocity vectors of the flow in the cross-section for (**a**) – heterogenous isotropic – S2 and (**b**.) heterogenous anisotropic – S3 conditions and (**c**.) conceptual diagram showing the three major flow systems in the investigated area (vertical exaggeration is 1:2). GF: groundwater flow

indicating the upwelling thermal water for the S3 scenario exhibits a residence time of 180 years, whereas those for the S2 scenario are 106 years. However, the thermal water may be older due as the particle tracking used in the simulation represents relatively small volumes of regional groundwater flow entering the discharge area, which may be influenced by the inflow of younger water from local systems.

As the regional flow paths occur below the local flow systems and continue downgradient, the average age of groundwater in the local flow systems is also influenced by

the vertical diffusion of water from the intermediate and regional systems (Fig. 8c and Fig. 9). The very low permeability of the Oligocene material, can result in groundwaters with longer residence times, some even greater than 10,000 years. Based on simulated streamlines, it can be estimated that some groundwaters may originate from beyond the model area to the east under thick Oligocene layers, that eventually discharge as thermal springs at Bled. The amount of water contributed by this component is likely to be small compared to the amount flowing from the western part of the model, but significant enough to prevent the regional groundwater flow component originating from the Triglav to pass beneath the Oligocene basin.

Discussion

The simulations support the assumption that the investigated groundwater flow pattern is induced by hydraulic head differences in the groundwater level (Fig. 9). Recharge occurs in areas with higher altitudes, with some proportion of groundwater drained in the form of local discharges. Additional streamlines representing regional groundwater systems flow to greater depths relative to local flow systems, where the influence of meteorological and hydrological conditions from the surface is noticeable. Streamlines indicate that the water infiltrates to a depth of over 2,000 m bgl and is heated along a gravity-driven flow. Groundwater discharge of regional flow systems occur at lower elevations. Consequently, the outflow of thermal groundwater corresponds to a regional flow system discharge area located near Lake Bled, where the lake represents the lowest surface elevation. The status of Lake Bled as a drainage area for both surface waters and regional groundwater flow is in accordance with Goldscheider et al. (2010). According to the Haitjema and Mitchell-Brucker (2005) the ratio (α; dimensionless decision criterion):

$$\alpha = \frac{RL^2}{mKHd} \tag{9}$$

For the site-specific values of the investigation area, the parameters are as follows: the average annual recharge rate $R = 2.4 \times 10^{-8}$ m s^{-1}, the average distance between hydraulic boundaries $L = 42{,}000$ m (assuming that the regional water divide is midway between two (regional) drainages); an aquifer shape factor $m = 8$, the horizontal hydraulic conductivity $K = 1 \times 10^{-6}$ m s^{-1}, the aquifer thickness $H = 2500$ m) and the maximum distance between the average surface water levels and the terrain elevation $d = 2386$ m. When substituting these values into Eq. (9), the dimensionless factor becomes 0.89. Generally, when $\alpha < 1$, the configuration of the groundwater table can be defined as recharge-controlled (where $\alpha > 1$ suggests the water table is topographically controlled). This has significant implications for the interpretation of regional groundwater flow patterns in th study area. It indicates that the dominant factor influencing the behaviour of the water table within the examined hydrogeological system is the quantity of water entering the system. This highlights the significance of recharge processes, in shaping the groundwater dynamics and transit times in the system. Furthermore, it also validate the phenomenon wherein recharge-controlled groundwater flow acts as a mechanism for transporting thermal water from deep underground reservoirs towards the surface, where it manifests as a thermal spring.

The outflow of thermal water takes place in the form of a thermal spring directly from the carbonate aquifer, or seeps into a glaciofluvial aquifer of Quaternary age (Fig. 7). The distribution of flow lines also indicates that in the eastern part of the model, some groundwater could originate from the east and flow under the Oligocene cover westwards, as far as the thermal water discharge zone similarly to BTK (Szijártó et al. 2021). Simulated ages of local groundwater flow in the unconfined carbonate aquifer region are of the order of 10 years to a maximum of a few tens of years, while in the case of thermal water, residence times can be expected to be up to 200 years. This result is consistent with groundwater residence times from other studies in alpine environments. The groundwater transit time of hydrothermal circulations is usually in the range of 10 to 1000 years (e.g., Vuataz 1982; Perello et al. 2001; Sonney 2010). However, in low permeability, siliciclastic aquifers, simulated residence times were found to be significantly higher, eg. for local systems > 1000 years.

Peclet number (Pe) values > 10 also shows that the Triassic carbonate system plays a key role in heat convection. Groundwater flow patterns determine the outflow of thermal water in Lake Bled, which are influenced by the geological conditions, i.e. geological structures, the boundary between the carbonate package (RS 1–RS 4) and Oligocene clay (RS 5) and their anisotropy. The simulations in this study did not account for a decrease in permeability with depth. While variations in permeability are a key consideration in certain hydrogeological environments, where significant decreases can occur with depth, this effect appears to be less pronounced in the Julian Alps. Although a slight decline in permeability likely exists with increasing depth, the presence of extensive cave systems exceeding 1 km in depth suggests that this decrease is not substantial enough to meaningfully influence the modeling results. High altitude topography has a marked effect on the distribution of the hydraulic head, therefore it can have a significant influence on the thermal regime (Domenico and Palciauscas 1973). Due to the predominantly advective heat transfer flow of groundwater, the temperature distribution in the system is

determined by forced convection, resulting in elevated water temperatures in the outflow area (Szijártó et al. 2019, 2021). According to the range of hydraulic conductivities for the investigated aquifer system, it is assumed that the conditions are not favourable for the development of free thermal convection. This can be proved also by calculating the Rayleigh number (Ra) – a theoretical criterion that determines whether or not thermal convection is likely to occur in the aquifer (Nield and Bejan 2017):

$$\mathrm{Ra} = \frac{g\alpha_r\rho_w c_w kL\Delta T}{\kappa\lambda} \tag{10}$$

where g is the acceleration due to gravity (9.81 m s^{-1}), α_r is the coefficient of the thermal expansion of water (2.4×10^{-4} $°C^{-1}$), c_w is the specific capacity of water (4185 J kg^{-1} K^{-1}), ρ_w is density (1000 kg m^{-3}), k is permeability (m^2), L is the height of the medium, ΔT is temperature difference, κ is water kinematic viscosity (m^2 s^{-1}), λ is thermal conductivity (W m^{-1} K^{-1}) and μ (kg m^{-1} s^{-1}) is the water dynamic viscosity. Assuming $\mu = 6.6\times10^{-4}$ kg m^{-1} s^{-1}, with $\lambda = 3$ W m^{-1} K^{-1}, a 3000 m deep carbonate system with $\Delta T = 33$ °C and critical $\mathrm{Ra}^* = 4\pi^2 \approx 40$ (Turcotte and Schubert 2002), then a minimum permeability of $k = 4.8\times10^{-15}$ m^2 (equivalent to $K = 1.2\times10^{-6}$ m s^{-1}) is required for the onset of free thermal convection. Considering the expected hydraulic conductivities of the examined geological units (ranging from 5×10^{-6} to 1×10^{-9} m s^{-1}), the conditions for the onset of free thermal convection are not optimal. This is mainly due to the low geothermal gradient in the investigated area. Moreover, Szijártó et al. (2019) suggested that increasing anisotropy hinders vertical flow and suppresses free thermal convection due to reduced vertical hydraulic conductivity.

The distribution of simulated groundwater temperature, illustrated by steady-state geothermal profiles expected in each section of the groundwater flow field can be described as follows (Figs. 7 and 8): (a) an isothermal profile in the recharge section characterised by lower temperatures, even at greater depths (over 2 km), (b) low-temperature horizontal flow at a depth where complete thermal equilibration has not yet occured, (c) elevated near-surface geothermal gradients in the outflow section, and (d) low-temperature outflow with potential heat storage beneath the confined part at a specific depth. The temperature distribution reflects the direction of groundwater flow: in the recharge area, the influence of cold groundwater resulting from infiltration extends throughout almost the entire thickness of the aquifer, resulting in a gradual temperature increase (from −1500 m asl) towards the bottom of the model. In this case, a negative heat anomaly can be assumed in the whole vertical section. In the outflow area, however, higher temperatures occur below the surface as the result of a positive thermal anomaly. In the outflow area, significant heat accumulation can be observed below and inside the low permeability sedimentary formations, which is especially pronounced under anisotropic conditions (Fig. 7). A comparison of scenarios S2 and S3 shows that anisotropy also has a significant effect on temperature distribution. Higher anisotropy forces topography-driven groundwater flow into the shallower region, which is consistent with the results of Szijártó et al. (2019).

The geological strata in the study area generally dip towards the NW-W and strike NE-SW, which, in a representative 3D model, could result in flow components along the strike direction. This possibility is supported by research worldwide, such as the work by Gleeson and Manning (2008), which emphasizes the significance of 3D topographic and hydrogeologic controls on regional groundwater flow in mountainous terrains. Their study demonstrates how the incorporation of 3D geometries in regional flow models is crucial for understanding complex flow systems, especially in areas with significant structural features. A 3D model for the Bled study area would likely capture flow components along the strike direction, potentially leading to a more nuanced representation of groundwater flow that includes NE or SW directions. However, for the purposes of this study, the primary focus was on the dominant flow patterns controlled by key boundary conditions within the cross-section which are predominantly lithological controlled (as shown in Fig. 4). The interpreted position of the groundwater table, along with the influence of topographic features and discharge locations such as springs, drives the flow predominantly in the E-W direction. Specifically, the hydraulic gradient west of Mt. Triglav is steeper than in the Krma Valley to the east, meaning that eastward flow is dominant in the modeled region. The springs west of Triglav, being at a higher elevation than those in the Krma Valley, indicate the presence of local outflow systems, and further reinforce the role of hydraulic gradients in controlling the main regional flow direction.

Simulations show that regional streamlines flow to depths of about 2 km below sea level, likely influenced by the position of the Permian-Carboniferous aquitard. This depth aligns with past and recent studies at similar areas (Rybach 1990; Bodri and Rybach 1998; Gallino et al. 2009; Luijendijk et al. 2020) and is considered significant for Alpine geology. The depth of thermal water circulation in the investigated system is largely controlled by the presence of low-permeability geological strata within the basement. While flow along the strike direction may be more accurately captured in a 3D model, the 2D approach used in this study provides a reasonable approximation for understanding the regional-scale flow dominated by the topographic gradients.

It is also visible from the simulations that the flow pattern is asymmetric, where the main discharge of thermal water is located in the area between the unconfined and confined sub-basins(Tóth et al. 2020). The findings of this

study are comparable to the findings of Mádl-Szőnyi and Tóth (2015) and Szijártó et al. (2021) for the Buda Karst, Hungary, despite the hydrogeological differences, especially in the basin length, depth, and geothermal gradient, flow pattern, temperature distribution, and the geographic location. The lateral and vertical distribution of temperature in the considered hydrological conditions is influenced by various factors. Based on the geothermal gradient of 10 °C km^{-1} in well Mmu-1/17, it is expected that the outflow of thermal water is the result of heating of groundwater at a depths of at least 1 km. In fact, the simulations indicate that the thermal water is heated at significantly greater depths, i.e. at depths below 2 km. The influence of forced thermal convection beneath unconfined karstified carbonate, where the cold water can directly infiltrate the depths and toward the discharge areas is due to the higher hydraulic conductivity of the Triassic aquifers and a high hydraulic gradient is due to water table configuration. The heat accumulation in the Oligocene layers east of Bled and the fractured zones associated with the Bled fault (Lapanje et al. 2009) are also important for the outflow of thermal water; however, in this confined aquifer, the heat transport mechanism can be interpreted as conductive. Recently, Szijártó et al. (2021) found that the influence of conductive faults on the heat flux and the recharge rate in the Buda Thermal Karst is insignificant when compared to the regional-scale temperature and Darcy flux fields. It is possible that the influence of hydraulically conductive faults on heat flux and recharge rates may vary depending on the specific geological and hydrogeological characteristics of a particular hydrogeological setting, which is why conductive faults will have to be taken into account in further simulations.

Conclusion

This paper exceptionally describes the regional groundwater flow pattern in an alpine carbonate aquifer system for the Bled (NW Slovenia) geothermal system. Groundwater flow and heat transport at the basin-scale were examined through three 2D numerical simulations in FEFLOW, which confirmed the occurrence of upwelling warm fluids due to the presence of a natural deep regional circulation system of adjoining mountainous (unconfined) and confined carbonate regions. The revealed pattern can be considered to be characteristic of the Alps and other similar mountainous systems worldwide, much like the well-known Buda Thermal Karst. The driving forces for groundwater circulation is primarily driven by differences in groundwater levels. So highly elevated carbonate areas are responsible for groundwater recharge, while discharge occurs in local or regional water table depressions. The varied topography and geology of the study area result in a hierarchical groundwater flow system, with shallow pathways reaching depths of a few hundred meters and deeper pathways extending up to 2 km within the regional or intermediate flow system.

The high relief of the study area causes significant lateral variations in the thermal regime. The predominance of advective groundwater flow means that temperature distribution is largely controlled by forced convection, with upwelling fluids emerging in regional outflow areas where thermal springs are located. Additionally, the geological boundary (i.e. the deepest topographic elevation) between the sub-basins of the unconfined Mesozoic carbonate and carbonates overlain by Oligocene clays determines the exact location of the upwelling thermal groundwater. The presence of the fault zone may enhance groundwater upwelling. A key role in the forced convection flow is played by a package of Triassic carbonate rocks, which have sufficiently favourable properties for advective heat transport. It can be concluded that the significant topographic differences in the alpine terrain control the configuration of the water table and therefore significantly affect the natural groundwater heat distribution and transit times within the system. These processes also play a critical role in sustaining groundwater-dependent ecosystems. Understanding basin-scale hydrogeological flow and heat transport processes is essential for effective water management in the Alpine region, especially in the context of a changing climate.

Acknowledgements The research was funded by the Slovenian Research and Innovation Agency (ARIS) throught the P1-0020 Groundwater and Geochemistry Research Program under the Young Researchers Programme (Grant No. 1000-19-0215) and a Bilateral State Scholarship for student mobility approved by the Tempus Public Foundation. The support of the National Multidisciplinary Laboratory for Climate Change, RRF-2.3.1-21-2022-00014 project is highly appreciated. The authors are also grateful to Sava Turizem d.d. for access to their archive of geothermal resources and monitoring data.

On behalf of all authors, the corresponding author states that there is no conflict of interest.

References

Al-Khoury R (2012) Computational Modeling of Shallow Geothermal Systems, 1st Edition. CRC Press. 254 pp. https://doi.org/10.1201/b11462

Andjelov M, Mikulič Z, Tetzlaff B, Uhan J, Wendland F (2016) Groundwater recharge in Slovenija: Results of a bilateral German-Slovenian Research project. Forschungszentrum Jülich GmbH, Jülich.

Andrič M, Massaferro J, Eicher U, Ammann B, Leuenberger MC, Martinčič A, Marinova E, Brancelj A (2009) A multi-proxy Late-glacial palaeoenvironmental recordfrom Lake Bled, Slovenia. Hydrobiologija 631:121–141. https://doi.org/10.1007/s10750-009-9806-9

ARSO (2021) Archive of weather observations. Agencija Republike Slovenije za Okolje-Slovenian Environmental Agency. http://meteo.arso.gov.si. Accessed 10 Jun 2021

Atanackov J, Jamšek Rupnik P, Jež J, Celarc B, Novak M, Milanič B, Markelj A, Bavec M, Kastelic V (2021) Database of Active Faults in Slovenia: Compiling a New Active Fault Database at the Junction Between the Alps, the Dinarides and the Pannonian Basin Tectonic Domains. Front Earth Sci 9. https://doi.org/10.3389/feart.2021.604388

Bavec M, Verbič T (2004) The extent of quaternary glaciations in Slovenia. In: Ehlers J, Gibbard PL (eds) Developments in quaternary science, vol 2, issue 1. Elsevier Science, pp 385–388. https://doi.org/10.1016/S1571-0866(04)80088-5

Bear J (1972) Dynamics of fluids in porous media. American Elsevier Publishing Company, New York, p 764

Bethke CM, Johnson TM (2008) Groundwater age and groundwater age dating. Annu Rev Earth Planet Sci 36:121–152

Bianchetti G, Roth P, Vuataz FD, Vergain J (1992) Deep groundwater circulation in the Alps: relations between water infiltration, induced seismicity and thermal springs: the case of Val d'Illiez, Wallis. Switzerland Eclogae Geolog Helvet 85(2):291–305

Bodri B, Rybach L (1998) Influence of topographically driven convection on heat flow in the Swiss Alps: a model study. Tectonophysics 291(1):19–27. https://doi.org/10.1016/S0040-1951(98)00028-6

Brenčič M (2003) Hydrogeological conditions of the Kroparica recharge area, Jelovica, Slovenia. Ljubljana, Geologija 46(2):281–306. https://doi.org/10.5474/geologija.2003.025

Buser S (1980) Explanatory book, sheet Celovec (Klagenfurt) L 33-53. Basic Geological Map of SFRJ 1(100,000):62. Zvezni geološki zavod, Beograd

Cuthbert MO, Gleeson T, Moosdorf N, Befus KM, Schneider A, Hartmann J, Lehner B (2019) Global patterns and dynamics of climate–groundwater interactions. Nat Clim Change 9(2):137–141. https://doi.org/10.1038/s41558-018-0386-4

Czauner Brigitta, Erőss Anita, Szkolnikovics-Simon Szilvia, Markó Ábel, Baják Petra, Trásy-Havril Tímea, Szijártó Márk, Szabó Zsóka, Hegedűs-Csondor Katalin, Mádl-Szőnyi Judit (2022) From basin-scale groundwater flow to integrated geofluid research in the hydrogeology research group of Eötvös Loránd University, Hungary. J Hydrol X 17:100142. https://doi.org/10.1016/j.hydroa.2022.100142

Dai X, Xie Y, Simmons CT, Berg S, Dong Y, Yang J, Love AJ, Wang C, Wu J (2021) Understanding topography-driven groundwater flow using fully-coupled surface-water and groundwater modeling. J Hydrol 594:125950. https://doi.org/10.1016/j.jhydrol.2020.125950

De Marsily G (1986) Quantitative hydrogeology. Academic press, New York, Groundwater Hydrology for Engineers, p 440

Diersch HJG (2013) FEFLOW: finite element modeling of flow, mass and heat transport in porous and fractured media. Springer, Heidelberg

Dzikowski M, Josnin JY, Roche N (2016) Thermal influence of an alpine deep hydrothermal fault on the surrounding rocks. Groundwater 54(1):55–65. https://doi.org/10.1111/gwat.12313

Domenico PA, Palciauskas VV (1973) Theoretical analysis of forced convective heat transfer in regional ground-water flow. Geol Soc Am Bull 84:3803–3814

Domenico PA, Schwartz FW (1998) Physical and chemical hydrogeology, 2nd edn. John Wiley & Sons, p 528

Forster C, Smith L (1989) The influence of groundwater flow on thermal regimes in mountainous terrain: A model study. J Geophys Res 94:9439

Freeze RA, Witherspoon PA (1967) Theoretical analysis of regional groundwater flow: 2. effect of water-table configuration and subsurface permeability variation. Water Resour Res 3(2):623–634

Gale L, Kolar-Jurkovšek T, Karničnik B, Celarc B, Goričan Š, Rožič B (2019) Triassic deep-water sedimentation in the Bled Basin, eastern Julian Alps, Slovenia. Ljubljana, Geologija 62(2):153–173. https://doi.org/10.5474/geologija.2019.007

Gallino S, Josnin JY, Dzikowski M, Cornaton F, Gasquet D (2009) The influence of paleoclimatic events on the functioning of an alpine thermal system (France): the contribution of hydrodynamic–thermal modeling. Hydrogeol J 17(8):1887–1900. https://doi.org/10.1007/s10040-009-0510-7

Gleeson T, Manning AH (2008) Regional groundwater flow in mountainous terrain: three-dimensional simulations of topographic and hydrogeologic controls. Water Resour Res 44:W10403. https://doi.org/10.1029/2008WR006848

Gleeson T, Marklund L, Smith L, Manning AH (2011) Classifying the water table at regional to continental scales. Geophys Res Lett 38:1–6. https://doi.org/10.1029/2010GL046427

Goldscheider N, Mádl-Szőnyi J, Erőss A, Schill E (2010) Review: thermal water resources in carbonate rock aquifers. Hydrogeol J 18(6):1303–1318. https://doi.org/10.1007/s10040-010-0611-3

Goričan Š, Žibret L, Košir A, Kukoč D, Horvat A (2018) Stratigraphic correlation and structural position of Lower Cretaceous flysch-type deposits in the eastern Southern Alps (NW Slovenia). Int J Earth Sci 107:2933–2953. https://doi.org/10.1007/s00531-018-1636-4

Haitjema HM, Mitchell-Bruker S (2005) Are water tables a subdued replica of the topography? Groundwater 43(6):781–786. https://doi.org/10.1111/j.1745-6584.2005.00090.x

Havril T, Molson JW, Mádl-Szőnyi J, (2016) Evolution of fluid flow and heat distribution over geological time scales at the margin of unconfined and confined carbonate sequences - A numerical investigation based on the Buda Thermal Karst analogue. Mar Pet Geol 78:738–749. https://doi.org/10.1016/j.marpetgeo.2016.10.001

Hilberg S, Riepler F (2016) Interaction of various flow systems in small alpine catchments: conceptual model of the upper Gurk Valley aquifer, Carinthia, Austria. Hydrogeol J 24:1231–1244. https://doi.org/10.1007/s10040-016-1396-9

Hubbert MK (1940) The theory of ground-water motion. J Geol XLVIII 8(1):785–944

Jiang XW, Wan L, Wang XS, Wang D, Wang H, Wang JZ, Zhang H, Zhang ZY, Zhao KY (2018) A multi-method study of regional groundwater circulation in the Ordos Plateau. NW China Hydrogeol J 26(5):1657–1668. https://doi.org/10.1007/s10040-018-1731-4

Jurkovšek B (1987) Explanatory book, sheet Beljak in Ponteba L 33-51, L 33-52. Basic Geological Map of SFRJ 1(100,000):58. Zvezni Geološki Zavod, Beograd

Kranjc T (2016) Speleološka analiza krasa med Viševnikom in Lipanco: Diplomsko delo (Speleological analysis of karst between

Viševnik and Lipanca). BSc thesis, University of Ljubljana, Slovenia
Kuniansky EL (2016) Simulating groundwater flow in karst aquifers with distributed parameter models – comparison of porous-equivalent media and hybrid flow approaches. Scientific Investigation Report (2016–5116):14. U.S. Geological Survey, Virginia. https://doi.org/10.3133/sir20165116
Lapanje A, Budkovič T, Rikanovič R, Rajver D, Rman N, Matoz T (2009) Hidrogeološke strokovne osnove za izkoriščanje termalne vode na Bledu (Hydrogeological expertise for the exploitation of thermal water in Bled). Geological Survey of Slovenia, Ljubljana
Lapanje A, Rman N (2009) Thermal and thermomineral water. In: Pleničar M, Ogorelec B, Novak M. (ed) The geology of Slovenia. Geological Survey of Slovenia, Ljubljana, Slovenia. p 553–560
Licour L (2014) The geothermal reservoir of Hainaut: the result of thermal convection in a carbonate and sulfate aquifer. Geol Belg 17(1):75–81
Lipsey L, Pluymaekers M, Goldberg T, van Oversteeg K, Ghazaryan L, Cloetingh S, Van Wees J-D (2016) Numerical modelling of thermal convection in the Luttelgeest carbonate platform, the Netherlands. Geothermics 64:135–151. https://doi.org/10.1016/j.geothermics.2016.05.002
López DL, Smith L (1995) Fluid flow in fault zones: analysis of the interplay of convective circulation and topographically driven groundwater flow. Water Resour Res 31(6):1489–1503. https://doi.org/10.1029/95WR00422
Lopez T, Antoine R, Kerr Y, Darrozes J, Rabinowicz M, Ramillien G, Cazenave A, Genthon P (2016) Subsurface hydrology of the Lake Chad Basin from convection modelling and observations. Surv Geophys 37:471–502. https://doi.org/10.1007/s10712-016-9363-5
Luijendijk E, Winter T, Köhler S, Ferguson G, von Hagke C, Scibek J (2020) Using thermal springs to quantify deep groundwater flow and its thermal footprint in the Alps and a comparison with North American orogens. Geophys Res Lett 47(22). https://doi.org/10.1029/2020GL090134
Mádl-Szőnyi J, Tóth A, (2015) Basin-scale conceptual groundwater flow model for an unconfined and confined thick carbonate region. Hydrogeol J 23(7):1359–1380. https://doi.org/10.1007/s10040-015-1274-x
Mádl-Szőnyi J, Batelaan O, Molson J, Verweij H, Jiang X-W, Carrillo-Rivera JJ, Tóth Á (2022) Regional groundwater flow and the future of hydrogeology: evolving concepts and communication. Hydrogeol J 31:23–26. https://doi.org/10.1007/s10040-022-02577-3
Magyar J, Kučina D, Kregar K, Kogoj D (2018) Metric representation of the bottom relief of Lake Bled: based on amateur hydrological measurements. Razgledi Muzejskega Društva Bled 10:140–149
Nield DA, Bejan A (2017) Convection in porous media, 5th edn. Springer, p 988. https://doi.org/10.1007/978-3-319-49562-0
Pasquale V, Chiozzi P, Verdoya M (2013) Evidence for thermal convection in the deep carbonate aquifer of the eastern sector of the Po Plain, Italy. Tectonophysics 594:1–12. https://doi.org/10.1016/j.tecto.2013.03.011
Perello P, Marini L, Martinotti G, Hunziker CJ (2001) The thermal circuits of the Argenterà Massif (western Alps, Italy): An example of low-enthalpy geothermal resources controlled by Neogene alpine tectonics. Eclogae Geol Helv 94:75–94
Placer L (1996) O Premiku Ob Savskem Prelomu Geologija (Displacement along the Sava Fault) 39(1):283–287. https://doi.org/10.5474/geologija.1996.011
Placer L (1999) Contribution to the macrotectonic subdivision of the border region between Southern Alps and External Dinarides. Geologija 41(1998):223–255
Placer L, Čar J (1998) Structure of Mt. Blegoš between the Inner and Outer Dinarides. Geologija 40:305–323
Rabinowicz M, Boulègue J, Genthon P (1998) Two and three-dimensional modeling of hydrothermal convection in the sedimented. Middle Valley segment, Juan de Fuca Ridge. J geophys Res 103(10): 24045–24065. https://doi.org/10.1029/98JB01484
Rajver D (2018) Gostota površinskega toplotnega toka = Surface heat flux density. In: Novak M, Rman N (eds) Geološki atlas Slovenije. Geološki Zavod Slovenije, pp 32–33
Rajver D, Adrinek S (2023) Overview of the thermal properties of rocks and sediments in Slovenia Geologija 66(1):125–150. https://doi.org/10.5474/geologija.2023.005
Rybach L, Eugster W, Griesser JC (1987) Die geothermischen Verhältnisse in der Nordschweiz (The geothermal conditions in northern Switzerland). Eclogae Geol Helv 80(2):531–534
Rybach L (1990) Determination of thermal water circulation depth, with examples from the Valaisan Alps, Switzerland. Proc. IAHS/IAH Symposium on Water Resources in Mountainous Regions, IAH Mémoires, XXII/1. Lausanne 1990:608–615
Rybach L (2009) Slowly moving thermal/mineral waters in deep crystalline basement. Environ Geol 58:1645–1651
Scanlon BR, Mace RE, Barrett ME, Smith B (2003) Can we simulate regional groundwater flow in a karst system using equivalent porous media models? Case study, Barton Springs Edwards aquifer, USA. J Hydrol 276(1–4):137–158. https://doi.org/10.1016/S0022-1694(03)00064-7
Serianz L (2016) Tri-dimensional Model of the Radovna Glacier from Last Glacial Period. Geologija 59(2):193–220. https://doi.org/10.5474/geologija.2016.011
Serianz L, Rman N, Brenčič M (2020) Hydrogeochemical Characterization of a Warm Spring System in a Carbonate Mountain Range of the Eastern Julian Alps. Slovenia Water 12(5):1427. https://doi.org/10.3390/w12051427
Serianz L, Rman N, Golobič I, Brenčič M (2022) Groundwater heat transfer and thermal outflow plume modelling in the Alps. Renew Energy 182:751–763. https://doi.org/10.1016/j.renene.2021.10.004
Sonney R, Vuataz FD (2009) Numerical modelling of alpine deep flow systems: a management and prediction tool for an exploited geothermal reservoir (Lavey-les-Bains, Switzerland). Hydrogeol J 17(3):601–616
Sonney R (2010) Groundwater flow, heat and mass transport in geothermal systems of a Central Alpine Massif: the cases of Lavey-les-Bains, Saint-Gervais-les-Bains, and Val D'Illiez. PhD Thesis, University of Neuchâtel, Switzerland, pp 111–130
Szijártó M, Galsa A, Tóth A, Mádl-Szőnyi J, (2019) Numerical investigation of the combined effect of forced and free thermal convection in synthetic groundwater basins. J Hydrol 572:364–379. https://doi.org/10.1016/j.jhydrol.2019.03.003
Szijártó M, Galsa A, Tóth A, Mádl-Szőnyi J, (2021) Numerical analysis of the potential for mixed thermal convection in the Buda Thermal Karst. Hungary J Hydrol Reg Stud 34:100783. https://doi.org/10.1016/j.ejrh.2021.100783
Šmuc A (2005) Jurassic and cretaceous stratigraphy and sedimentary evolution of the Julian Alps, NW Slovenia. Založba ZRC/ZRC Publishing, Ljubljana. https://doi.org/10.3986/9789612545147
Taillefer A, Guillou-Frottier L, Soliva R, Magri F, Lopez S, Courrioux G, Millot R, Ladouche B, Le Goff E (2018) Topographic and Faults Control of Hydrothermal Circulation Along Dormant Faults in an Orogen. Geochem Geophys 19:1–2. https://doi.org/10.1029/2018GC007965
Thiébaud E, Gallino S, Dzikowski M, Gasquet D (2010) The influence of glaciations on the dynamics of mountain hydrothermal systems: numerical modeling of the la Léchère system (Savoie, France). Bull Soc Geol Fr 181(4):295–304. https://doi.org/10.2113/gssgfbull.181.4.295
Tóth J (1962) A theory of groundwater motion in small drainage basins in central Alberta. Canada J Geophys Res 67(11):4375–4387

Tóth J (1963) A theoretical analysis of groundwater flow in small drainage basins. J Geophys Res 68:4795–4812
Tóth J (1995) Hydraulic continuity in large sedimentary basins. Hydrogeol J 3(4):4–16
Tóth J (2009) Gravitational systems of groundwater flow theory, evaluation, utilization. Cambridge University Press, Cambridge
Tóth A, Galsa A, Mádl-Szőnyi J, (2020) Significance of basin asymmetry and regional groundwater flow conditions in preliminary geothermal potential assessment – Implications on extensional geothermal plays. Glob Planet Change 195:103344. https://doi.org/10.1016/j.gloplacha.2020.103344
Tóth Á, Baják P, Szijártó M, Tiljander M, Korkka-Niemi K, Hendriksson N, Mádl-Szőnyi J (2023) Multimethodological Revisit of the Surface Water and Groundwater Interaction in the Balaton Highland Region—Implications for the Overlooked Groundwater Component of Lake Balaton. Hungary Water 15(6):1006. https://doi.org/10.3390/w15061006
Turcotte DL, Schubert G (2002) Geodynamics - application of continuum physics to geological problems. Cambridge University Press, Cambridge, p 456
VDI (2012) Thermische Nutzung des Untergrundes (Guideline for thermal use of the underground). Vdi-richtlinie 4640, Verein Deutscher Ingenieure (VDI) - Gesellschaft Energietechnik, Germany
Verbovšek T (2008) Hydraulic conductivities of fractures and matrix in Slovenian carbonate aquifers. Geologija 51(2):245–255. https://doi.org/10.5474/geologija.2008.025
Volpi G, Magri F, Frattini P, Crosta GB, Riva F (2017) Groundwater-driven temperature changes at ther-mal springs in response to recent glaciation: Bormio hydrothermal system, Central Italian Alps. Hydrogeol J 25:1967–1984. https://doi.org/10.1007/s10040-017-1600-6
Vuataz FD (1982) Hydrogéologie, géochimie et geothermal des eaux thermales de Suisse et des régions limitrophes [Hydrogeological, geochemical and geothermal characteristics of thermal waters in Switzerland and the bordering Alpine areas]. Matér Géol Suisse Sér Hydrol 29:174